JOURNAL OF MATERIALS SCIENCE 29 (1994) 2087–2094

Crystallization of glasses obtained by recycling goethite industrial wastes to produce glass–ceramic materials

M. PELINO*, C. CANTALINI, F. VEGLIO'
Department of Chemistry, Chemical Engineering and Materials, University of L'Aquila, 67040 Monteluco di Roio, L'Aquila, Italy

P. P. PLESCIA
CNR, Istituto Trattamento Minerali, via Bolognola 7, 00138 Roma, Italy

Goethite waste, originated in the hydrometallurgy of zinc, was characterized and recycled, in combination with raw materials, for producing glass–ceramic (GC) materials. Four base compositions were prepared with an Fe_2O_3 content ranging from 15 to 25 wt%. The mixtures were melted at 1400–1450 °C and quenched to obtain the glass. The nucleation and crystallization temperatures and the activation energy of the crystallization process were determined by differential thermal analysis. The glass samples were nucleated at 660 °C for times ranging from 1 to 4 h and crystallized at 800–900 °C for 1 to 4 h. X-ray diffraction and fluorescence analysis were performed on the glasses and GC samples and the crystalline phases characterized. The percentage of crystallinity was determined as a function of the temperature and duration of the thermal treatment. The fractional factorial experimental approach was carried out on the 20 wt% Fe_2O_3 composition with the aim of evaluating the influence of the nucleation temperature and time, the crystallization temperature and time and the presence of a reducing agent on the glass devitrification process.

1. Introduction

Goethite (FeOOH) is an iron-rich toxic waste that arises in the roast–leach–electrowin process for producing zinc concentrates. The iron is removed from the zinc leach liquor, before it is further purified by electrolysis, by hydrothermal precipitation at the proper temperature and pH. The goethite waste contains considerable quantity of heavy metals (Pb, Zn, Cd, Cu, Ni, As) and for this reason is considered a "toxic residue". About 120 000 t was the evaluation of the Italian zinc-industry production of goethite waste in 1990. Other zinc-hydrometallurgy residues (i.e. jarosite and haematite) are produced in large quantities in the European Community and, in the same year, the total amount of zinc-production residues was computed as 600 000 t.

At present, the disposal of these wastes represents an acute environmental problem and is generating serious social and economic difficulties for European zinc companies, resulting in an increase in metal cost production. The environmental protection legislation of the European Countries is concerned with the level of toxic metals in the slurry and will not allow further storage of the waste in ponds, even if especially conceived for this purpose. With different emphasis, European Countries are bringing increasing pressure on their zinc industries either to seek other methods of iron elimination which will produce an environmentally benign residue, or to treat the waste to recover the valuable elements, such as Zn and Pb, and to produce a final residue acceptable for disposal.

Several methods have been proposed in order to reduce or eliminate the problem of the waste. In one of these, the waste is mixed with lime and treated for several hours in rotary furnace between 900 and 1200 °C; the final product is an inert material obeying the existing regulations for disposal of wastes. The total cost of this process is about $ 200 per tonne. The waste can be sealed in a cement mix to make it inert and then somehow recycled in the building industry. The waste can be reprocessed to recover the valuable elements and compounds (SO_2) and recycle the iron oxide in the steel industry.

The experimental results presented in this work are part of a project, supported by the European Community under the programme "Raw Materials and Recycling", aimed at recycling the highest quantity of goethite waste to produce glass–ceramic (GC) materials with properties suitable for the commercial exploitation. Goethite waste produced in an Italian zinc plant was chemically and physically characterized, mixed with other industrial residues and raw materials, melted, vitrified and then crystallized by means of suitable thermal treatments. Preliminary fractional

* To whom all correspondence should be addressed.

0022–2461

factorial design was performed to evaluate the effects of different factors on the glass crystallization process.

No information is available in the literature on the specific topic but the scientific investigation of the project is based on the science and technology of GCs produced from molten natural rocks, foundry slags and other industrial wastes and described in detail in the literature [1–3]. The project follows the current tendency to inglobe toxic and radioactive wastes in a glass or glass–ceramic matrix, as highlighted in a recent survey of the GC world patent market [4].

2. Experimental procedure

The experimental procedure employed for the chemical and physical characterization of the goethite red mud is reported elsewhere [5–7]. Table I summarizes the chemical composition of the waste. The weight loss of the dried goethite was evaluated in the 0–1400 °C temperature range by simultaneous thermal analysis (STA) at a heating rate of 10 °C min^{-1}. The results are depicted in Fig. 1.

In the thermal gravimetry (TG) trace, about 8% of the weight loss occurred in the 100–400 °C range, due to the decomposition of goethite to yield haematite (Fe_2O_3). The sharp endothermic peak at 767 °C in the differential thermal analysis (DTA) trace was attributed to the decomposition of sulphates and carbonates. Their decomposition starts at about 700 °C and ends at 1350 °C with a weight loss of 15.8%. The total weight loss in the whole investigated temperature range was 23.9%. Fourier transform infrared (FTIR) analysis of the gases evolved from the STA crucible highlighted that 10.2% was constituted by SO_2, the rest being water and CO_2.

With the aim of removing the soluble zinc sulphates, the goethite mud was washed several times with distilled water. With this treatment about 50% of the sulphates were removed from the waste. The filtered goethite was dried and then mixed with sand, feldspath, limestone, MgO and Al_2O_3, to obtain different compositions with Fe_2O_3 contents equal to 15.0% (Fe15/01), 17.0% (Fe17/01), 20.0% (Fe20/01) and 25% (Fe25/01). 2.0% of TiO_2 was added to all compositions to promote heterogeneous nucleation; to the Fe20/01 composition sugar (sucrose) was introduced in about stoichiometric quantity, to reduce Fe^{3+} to Fe^{2+} and facilitate the precipitation of magnetite (Fe_3O_4) and titano-magnetite (Fe_2TiO_4). This mixture is indicated as Fe20/01S. The investigated compositions are listed in Table II.

Fusion was performed in an alumina crucible at 1400–1450 °C, since this material is hardly affected by aggressive batch compositions [8]. Quenching of the molten batch to obtain the glass was performed on preheated graphite moulds; this relatively slow quen-

TABLE I The chemical composition of dried goethite waste

Oxide	Fe_2O_3	ZnO	PbO	SiO_2	CaO	Al_2O_3	CuO	As_2O_3	NiO	CdO	Na_2O	LOI
Wt %	51.3	13.3	6.27	2.91	0.1	0.7	0.50	0.3	0.3	0.1	0.1	23.9

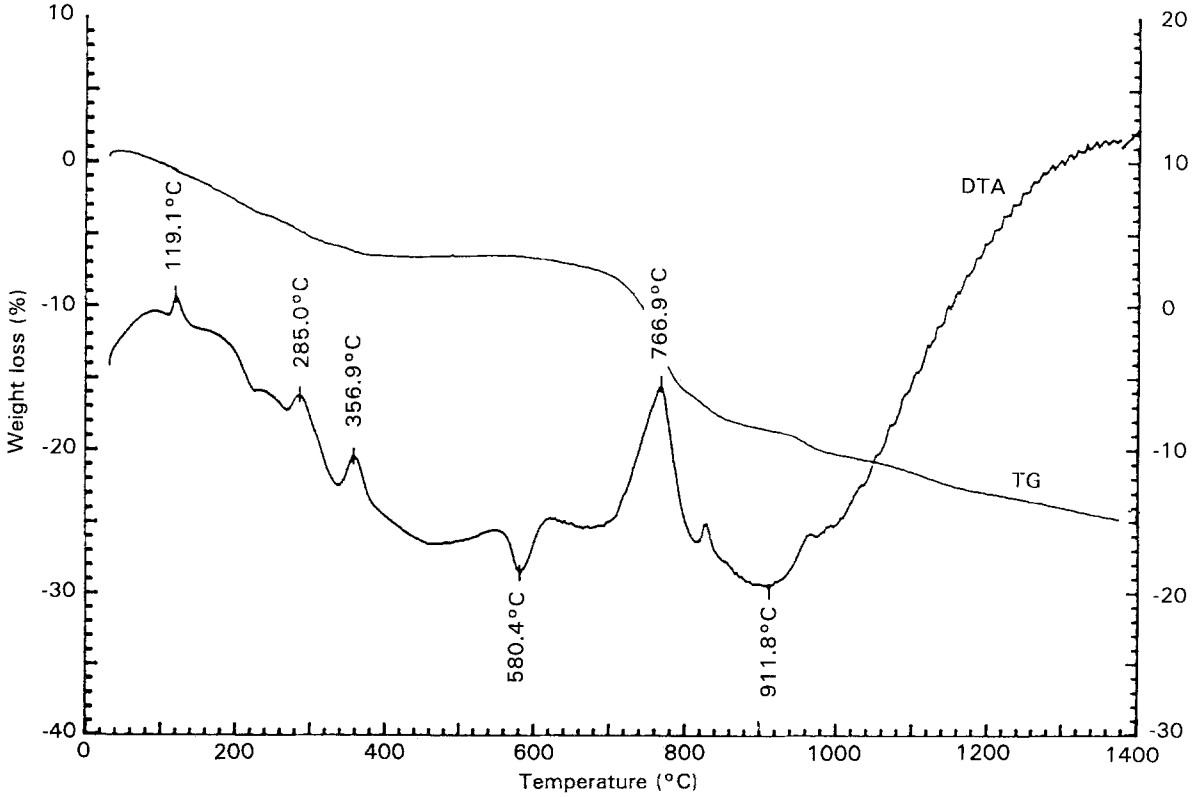

Figure 1 Thermal gravimetry (TG) and differential thermal analysis (DTA) of the goethite waste.

TABLE II Chemical compositions (wt%) of the goethite samples

Oxide	Fe15/01	Fe17/01	Fe20/01	Fe25/01
SiO_2	44.00	42.44	51.00	44.00
Al_2O_3	14.00	10.00	0.27	0.34
Fe_2O_3	15.00	17.00	20.00	25.00
MgO	8.00	9.00	4.00	4.00
CaO	9.00	10.00	10.00	10.00
Na_2O	2.00	2.00	4.63	4.40
TiO_2	2.00	2.00	2.00	2.00
PbO	2.01	2.28	2.44	3.05
K_2O	0.02	0.02	0.02	0.02
SnO_2	0.02	0.02	0.02	0.02
CuO	0.15	0.17	0.18	0.22
ZnO	4.27	4.84	5.18	6.47
As_2O_3	0.09	0.11	0.13	0.14
NiO	0.09	0.11	0.13	0.14
CdO	0.03	0.03	0.03	0.04

ching was chosen to promote glass formation and to induce lower stresses in the glass structure. All the glasses produced were annealed at 600 °C for 30 min in order to remove any residual stress and improve the final properties of the glass–ceramic.

After annealing, samples of each glass were analysed by X-ray diffraction (XRD) to ensure that no crystallization occurred during the quenching and annealing. XRD was also employed to evaluate the amorphous and crystalline fractions in the GC. These determinations were carried out by means of CuK_α radiation from a tube operating at 35 kV and 40 mA with 10 s scanning time; a graphite crystal monochromator was used. The level of instrumental noise was limited by means of specially designed quartz sample holder.

X-ray fluorescence analysis confirmed that no modifications occurred in the composition during the melting operation. This technique was also employed to determine the ratio Fe^{3+}/Fe^{2+} in the glasses.

3 Results

3.1. Thermal effects in the crystallization of glasses

The crystallization of a supercooled liquid is controlled by two factors: the first is the nucleation rate, i.e. the number of nuclei formed in a unit of volume per unit of time; the second is the rate of crystal growth, i.e. the rate of shift of the crystalline phase boundary in the liquid. The higher is the cooling rate of the melt across the temperature of maximum nucleation and crystal growth rate, the greater is the possibility of glass formation. By subsequent thermal treatment of the glass, the nucleation and crystallization can take place in a controlled manner leading to the formation of crystalline phases throughout the bulk of the sample.

In the kinetics of crystallization of glasses, the nucleation process acquires particular importance because an efficient rate of nucleation greatly affects the final properties of the glass–ceramic. The formation of nuclei throughout the bulk of the glass is usually characterized as homogeneous when the composition and crystal structure of the nucleus are the same as those of the crystallized glass, and as heterogeneous when the nucleating phase is chemically and structurally different from the phase (or phases) precipitating during the crystallization. The critical radius of the nuclei, r_c, is related to the liquid–crystal interfacial energy, γ, and the difference in free energy between the liquid and the solid phases, ΔG_v, through the expression

$$r_c = -\frac{2\gamma}{\Delta G_v} \quad (1)$$

The higher the degree of supercooling, the greater the ΔG_v that represents the driving force for the nucleation.

DTA (or differential scanning calorimetry, DSC) is a powerful tool in detecting and analysing the thermal effect produced when the formation of crystallites is taking place in a glass matrix. Fig. 2 shows the DTA traces of samples Fe15/01, Fe17/01, Fe20/01, Fe20/01S and Fe25/01, performed at 10 °C min^{-1} heating rate. The first two samples, Fe15/01 and Fe17/01, show sharp crystallization peaks at 887 and 856 °C, respectively, while a broad trace is obtained for the Fe20/01, Fe20/01S and Fe25/01 samples. The addition of the reducing agent, introduced into batch Fe20/01S to increase the ratio FeO/Fe_2O_3 and improve the nucleation of magnetite and the crystallization of the glass, did not noticeably affect the shape of the DTA trace.

The exothermic peak corresponding to the nucleation of magnetite was not detected by DSC, since the amount of heat evolved is below the sensitivity of the instrumentation. The temperature of maximum nucleation was therefore inferred by performing, on the Fe17/01 glass, nucleation at different temperatures in the range 650–750 °C, followed by crystallization at

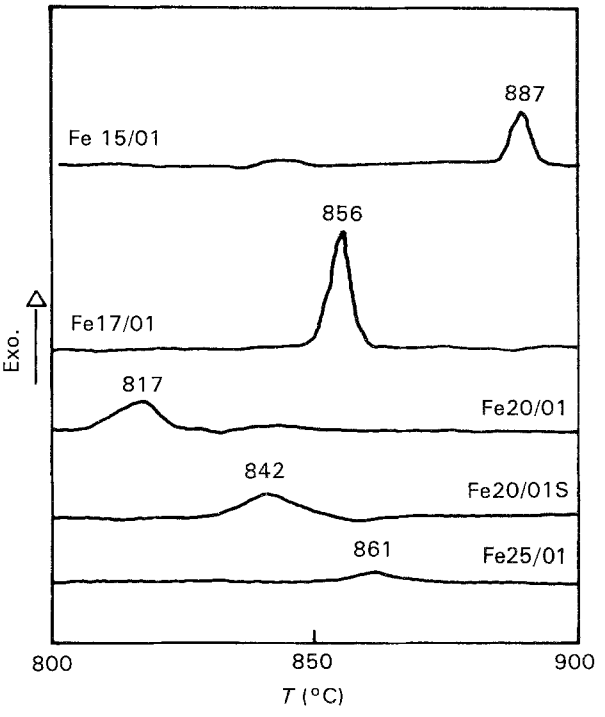

Figure 2 Crystallization DTA traces of Fe15/01, Fe17/01, Fe20/01, Fe20/01S and Fe25/01 glasses at 10 °C min^{-1} heating rate.

860 °C for 1 h; the sample with the highest percentage of crystalline phase indicated the nucleation temperature. It transpired to be 660 °C. A closely similar value of nucleation temperature was obtained for glasses with an oxide composition similar to the ones investigated here [9].

By carrying out DTA on samples with different grain sizes, bulk and surface crystallization mechanisms can be distinguished: if crystallization of the glass powder occurs mainly on the surface of the particles, a fine granulometry will favour the phenomenon more than a coarse one. In the latter case the crystallization peak will be detected at a higher temperature. DTA performed on the five glass compositions, each with different granulometry, showed no significant shift in the position of the crystallization peak and confirmed the bulk mechanism.

3.2. The activation energy (E_a) of the glasses

By performing DTA at different heating rates (usually between 2 and 40 °C min^{-1}) on the same type of glass, the activation energy E_a of the crystallization process can be evaluated. E_a can be regarded as the sum of the energy of nucleation of the nuclei (E_n) and the energy of crystal growth (E_g) of the crystallites. The lower E_a, the more efficient is the crystallization of the glass to obtain GC materials.

For the evaluation of E_a, DTA was carried out at different heating rates for the Fe15/01, Fe20/01 and Fe20/01S samples. The parameters employed in the calculation of the activation energy are β, the heating time (°C min^{-1}) and T_p, the crystallization temperature (K). In Fig. 3 are shown the best lines obtained by depicting logβ versus $1/T$ through least-squares analysis of the data. E_a is than obtained from the slope of the straight lines by means of the relation

$$\log\beta = -\frac{E_a}{19.1T_p} + \text{const.} \quad (2)$$

The activation energies for the crystallization of the glass were determined as $E_a = 440 \pm 25$, 270 ± 25 and 250 ± 25 kJ mol^{-1} for Fe15/01, Fe20/01 and Fe20/01S, respectively. The error given is an overall estimation of the associated uncertainties.

3.3. Characterization of crystalline phases in the GC

The XRD spectra of the GC, obtained by 180 min treatment at 860 °C, contain various phases identified as clinopyroxene, olivine, magnetite and titano-magnetite. They were shown and discussed in previous papers [5]. The crystalline fraction developed in the GC as a function of the thermal treatment time was calculated by the XRD spectra using the relation

$$\%\ \text{Cryst. phase} = 100\frac{C}{C + A} \quad (3)$$

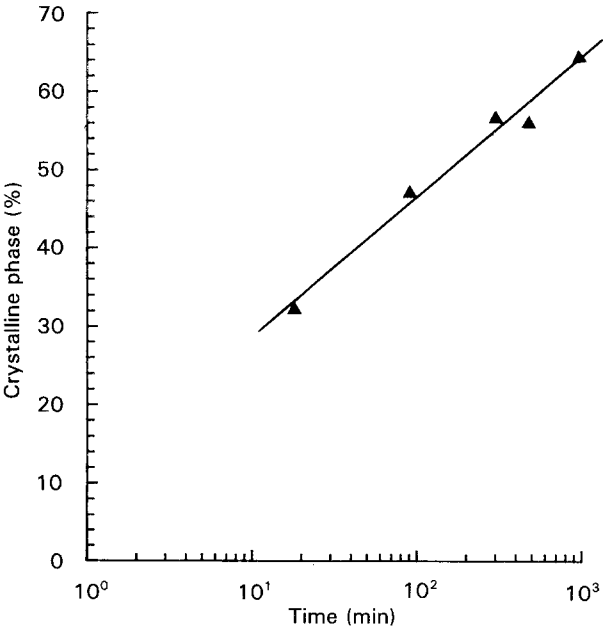

Figure 4 Percentage of crystalline phase as a function of treatment time (in log scale) for Fe17/01.

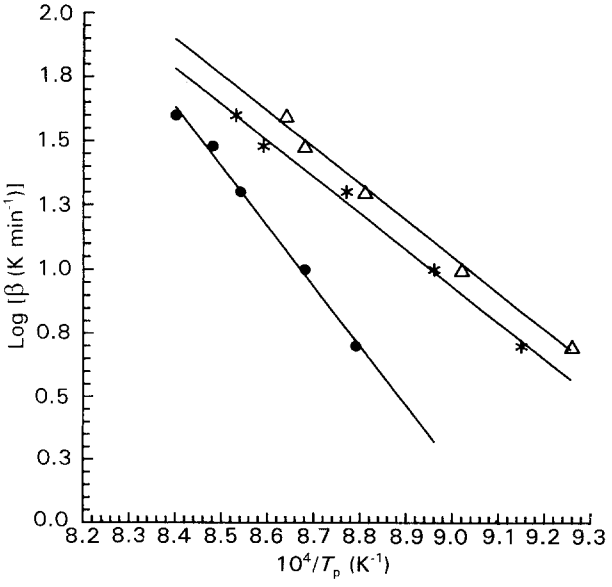

Figure 3 Activation energy plots of (●) Fe15/01, (△) Fe20/01 and (∗) Fe20/01S GCs.

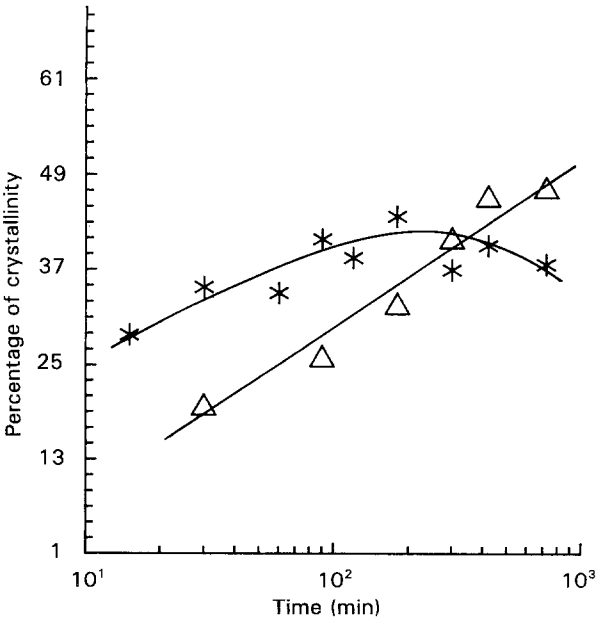

Figure 5 Percentage of crystalline phase as a function of treatment time (in log scale) for (△) Fe20/01 and (∗) Fe20/01S.

where C represents the integral of the discrete crystalline spectrum and A the integral of the continuous amorphous spectrum. The results for Fe17/01, Fe20/01 and Fe20/01S are shown in Figs 4 and 5. They highlight the fact that the crystallization is more efficient for sample Fe17/01 than for Fe20/01, being 61% the maximum value obtained in the first case and 54% in the latter. The addition of sugar to Fe20/01 improves the crystallization at low times while it produces a negative effect for times longer than 180 min.

A possible explanation of this behaviour is that the presence of the reducing agent improves the nucleation of magnetite so that more stable nuclei are formed at the nucleation temperature with a critical radius that is a function of the degree of supercooling, i.e. the ΔG_v value, according to Equation 1. When the temperature is raised to the crystallization temperature some nuclei will become unstable and will disappear. The instability of nuclei due to the diminishing of ΔG_v, i.e. the increasing of critical radius, becomes more evident when the duration of the thermal treatment is prolonged.

Fig. 6a and b show pyroxene grains identified by scanning electron microscopy (SEM) on the etched surface of Fe20/01 and Fe20/01S GC samples, respectively. The inset on the upper left side of Fig. 6b is the back-scattered electron SEM image. The two pictures highlight noticeable differences in the typical dendritic form of pyroxene: Fig. 6b shows well-developed grains, uniformly distributed and with 1 to 10 μm diameter; the sample without reducing agent, Fe20/01 in Fig. 6a, shows smaller and fewer grains with a simple dendritic structure. Both samples were crystallized at 860 °C for 180 min. Fig. 6c shows the development of an Fe20/01S pyroxene grain after 16 h thermal treatment. The measured ratios Fe^{3+}/Fe^{2+} were 12.0 and 8.7 for Fe20/01 and Fe20/01S, respectively.

Fig. 7 is the X-ray fluorescence spectrum of a grain and shows the presence of the K_α peak at about 8.6 keV, of the zinc replacing Fe and Ca in the structure of the pyroxene. The emission radiations, of the other heavy metals present in the goethite mud, and inglobed in the crystal structure, were also detected.

With respect to the diopsitic-hedembergitic pyroxene $(Ca, Fe)_2Si_2O_6$, the presence of zinc in the monoclinic structure, with a smaller ionic radius than Fe^{2+} and Ca^{2+}, will produce a reduction of the unit cell parameters. Compared to the cell volume of the hedembergitic, $0.4528 + 0.0002\ nm^3$ [10], the value found in this study by XRD analysis was $0.4513 + 0.0001\ nm^3$ for Fe20/01S GC. This cell-volume reduction is in agreement with the percentage of zinc in the GC.

3.4. Fractional factorial design (FFD) on crystallization thermal treatment

With the aim of evaluating the influence of the nucleation and crystallization process, i.e. time and temperature of thermal treatment as well as the influence of the reducing agent (sugar) in the batch, a fractional factorial experimental preliminary approach was car-

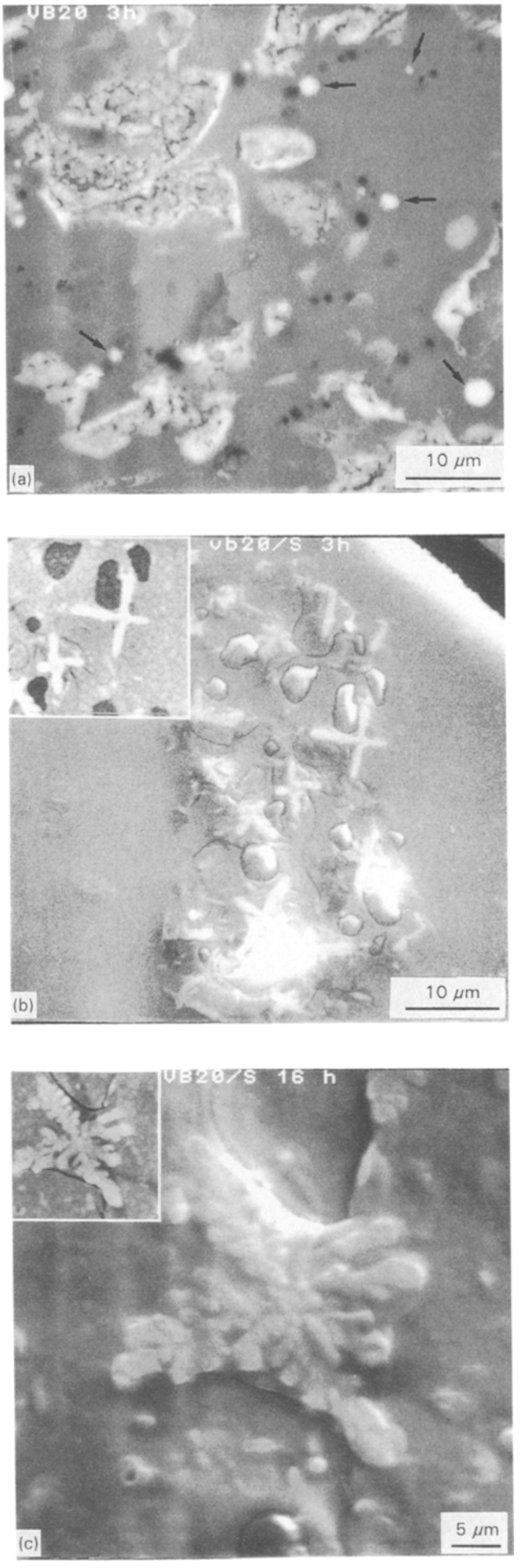

Figure 6 Pyroxene grains of (a) Fe20/01 after 3 h thermal treatment, (b) Fe20/01S after 3 h thermal treatment, (c) Fe20/01S after 16 h thermal treatment.

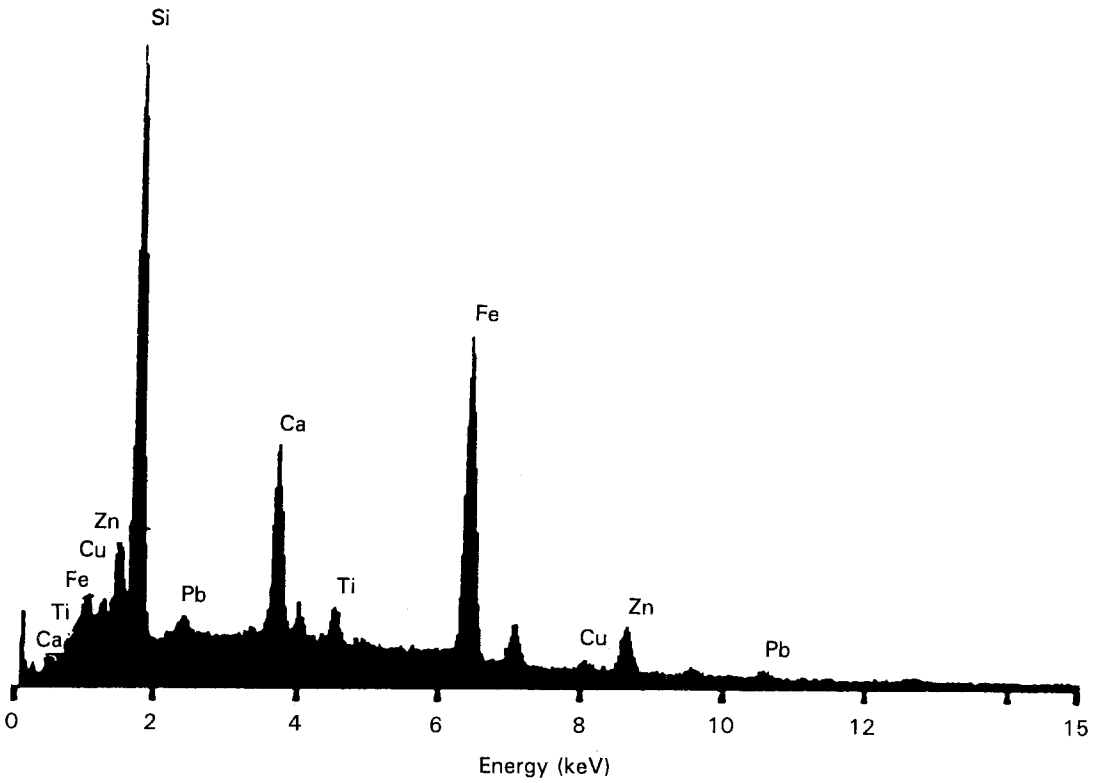

Figure 7 X-ray fluorescence of a pyroxene grain.

TABLE III Factors and levels employed in FFD

Code	Factor	Low	High
A	Nucleation time (h)	0.30	4
B	Nucleation temperature (°C)	630	700
C	Crystallization time (h)	0.30	3
D	Crystallization temperature (°C)	800	900
E	Reducing carbon	No	Yes

ried out on the Fe20/01 and Fe20/01S GC compositions. This methodology is very helpful both in experimental planning and in statistical interpretation of the results [11]. In this manner it is possible to arrange an orthogonal experimental plane in which one can evaluate the main effects and the interactions, independently, among the factors investigated. The presence of an interaction or synergism indicates that there is a change in the effect of a factor, (i.e. nucleation time) which changes the levels of yet another factor (i.e. reducing carbon).

Five different factors, i.e. the nucleation and crystallization temperatures and times and the reducing agent, each of them investigated at two different levels, were combined through FFD. Instead of the 32 experiments required for the full factorial design, 16 tests were carried out in different experimental conditions. The levels of each factor are reported in Table III. Reduction of the experimental plane (from 32 to 16 tests in this case) always generates confusion among the main effects and their interactions. The proper selection of the defining contrast (DC), which identify the fractional design, allows one to determine the confusion plane and the reduction of the full factorial design [11].

The defining contrast utilized in the experimental design was I,-ABCDE. With this design all the main effects are not confused with two interactions, and these are confused only with three interactions that generally are not important. For example, utilizing the multiplication rules

$$A \times A = A^2 = I$$
$$A \times ABCD = A^2BCD = BCD$$

with DC = I,-ABCDE, the effect of A is confused only with -BCDE interaction; the effect AB is confused with -CDE interaction, etc..

The experimental error was $3(\%)^2$ with five degrees of freedom. This value was obtained by performing six thermal treatments of the FFD, twice. The investigated surface response of the process was the percentage of crystalline phase as evaluated by XRD analysis of the GC samples, through Equation 3. Yates' notation was utilized in this work to name each experimental condition tested. Table IV reports the fractional factorial parameters employed in each experiment with the corresponding value of surface response, i.e. the percentage of crystalline phase.

The experiments indicated with an asterisk relate to Fe20/01S, with reducing agent. The analysis of variance ANOVA is reported in Table V with the estimated significance levels of the main effects and interactions. The ANOVA is also shown in Fig. 8. The figure reports the effects and interactions with a significance higher than 90%. As can be seen, some of these effects and interactions show a positive influence upon crystallization. The higher their values, the more effective they are in promoting the crystallization process of the glass. The same consideration applies in the negative sense. On the basis of the results shown in Fig. 8, the following assertions can be made:

TABLE IV Experimental conditions in FFD (asterisk indicates the presence of reducing agent)

	Nucleation time, θ_n (h)	Nucleation temperature T_n (°C)	Crystallization time, θ_c (h)	Crystallization temperature (°C)	Crystalline phase (%)
1	2.00	630	0.30	800	29.4
2	4.00	700	0.30	800	32.4
3	4.00	630	3.00	800	32.6
4	2.00	700	3.00	800	42.5
5	4.00	630	0.30	900	39.0
6	2.00	700	0.30	900	41.1
7	2.00	630	3.00	900	33.4
8	4.00	700	3.00	900	27.9
1*	4.00	630	0.30	800	26.1
2*	2.00	700	0.30	800	29.9
3*	2.00	630	3.00	800	32.2
4*	4.00	700	3.00	800	31.1
5*	2.00	630	0.30	900	36.3
6*	4.00	700	0.30	900	45.8
7*	4.00	630	3.00	900	34.8
8*	2.00	700	3.00	900	53.5

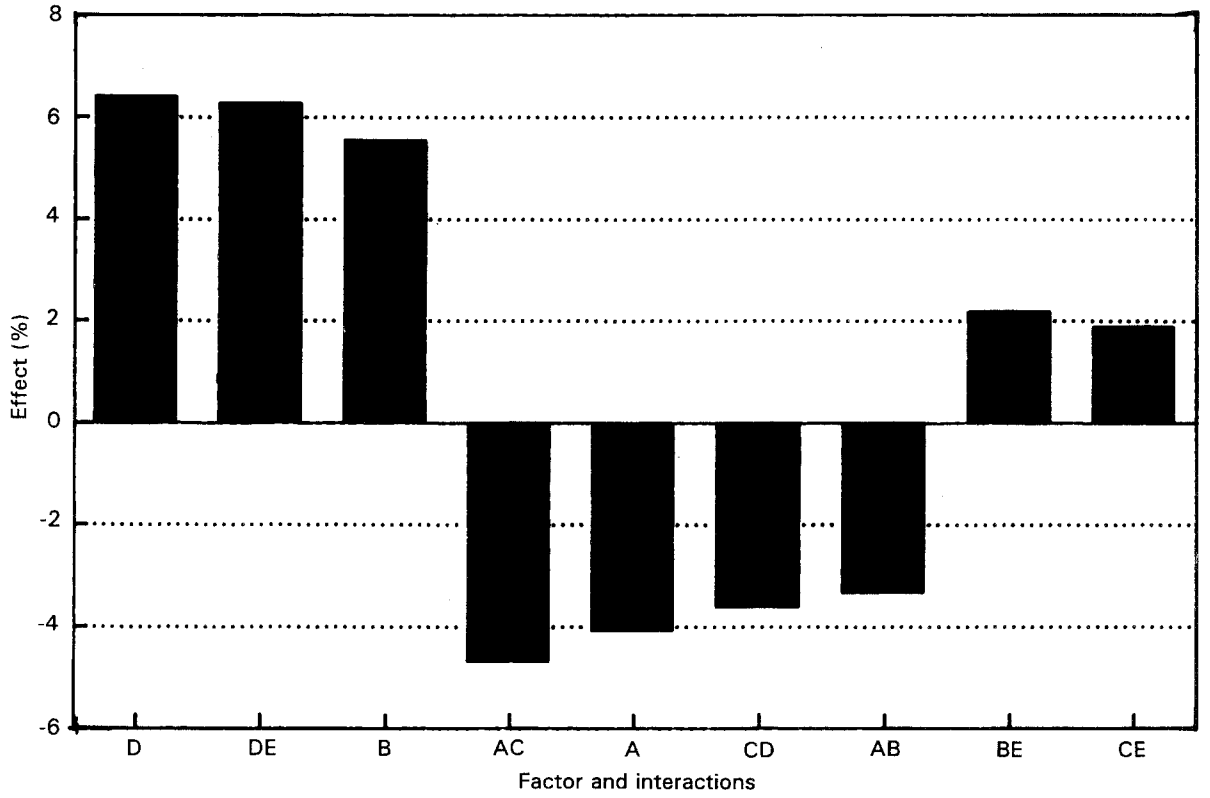

Figure 8 Fractional factorial design: effects as a function of the factors and their interactions.

1. The maximum effect on the crystallization of the glass is attained by the crystallization temperature (D) and the nucleation temperature (B); higher crystallization is obtained by increasing D and B factors in the range investigated. The result agrees with thermodynamic studies on the nucleation and crystallization of glasses [3]. An important role is also played by interaction between the crystallization temperature and the reducing agent (DE). As previously pointed out, the reduction of Fe^{3+} to Fe^{2+} favours the precipitation of magnetite as a nucleating agent and increases the influence of the crystallization thermal treatment.

2. The effect of the crystallization time (C) is positive but only with 85.6% significance, and is not included in Fig. 8. This result demonstrates that when efficient nucleation is obtained and the crystallization temperature is accurately determined, the crystallization time is of minor importance in the crystallization of glasses. Furthermore, in view of a possible industrial development of the process, a shorter period of crystallization at high temperature will result in considerable energy saving.

3. The nucleation time (A) and its interaction with the crystallization time (AC) have a negative effect. This means that a longer nucleation period adversely affects the number of nuclei formed. Small negative effects on the percentage of crystalline phase are also shown by the interactions between crystallization time

TABLE V ANOVA analysis: effects and significance levels of the investigated factors

Run	Code	% Cryst.	Effects	MS	Sign. (%)
1	1	29.4	–	–	–
2	ae	26.1	A = − 4.13	68.1	99.5
3	be	29.9	B = + 5.55	123.2	99.86
4	ab	32.4	AB = − 3.38	45.5	98.86
5	ce	32.2	C = + 1.50	9.0	85.62
6	ac	32.6	AC = − 4.73	89.3	99.72
7	bc	42.5	BC = − 0.00	0.0	–
8	abce	31.1	DE = + 6.28	157.5	99.92
9	de	36.3	D = + 6.40	163.8	99.93
10	ad	35	AD = − 1.18	5.5	76.71
11	bd	41.1	BD = + 1.65	10.9	88.49
12	abde	45.6	CE = + 1.88	14.1	91.73
13	cd	33.4	CD = − 3.65	53.3	99.16
14	acde	34.6	BE = + 2.18	18.9	94.63
15	bcde	53.5	AE = + 0.50	1.0	41.13
16	abcd	27.9	E = + 1.88	14.1	91.73

and temperature (CD) and nucleation time and temperature (AB).

4. The presence of the reducing agent (E) generates a positive effect as well as its interaction with the crystallization temperature (DE), nucleation time (BE) and crystallization time (CE).

4. Conclusions

In the compositions investigated in this study up to 0.5 kg of dried goethite waste was recycled per kg of glass produced (Fe25/01). The cooling rate used to obtain the amorphous phase is comparable to the industrial cooling conditions used in the production of glasses.

The precipitation of magnetite and titano-magnetite as nucleating agents promotes the formation of crystalline phases through a controlled thermal treatment. The crystalline phases and the crystalline/amorphous phase ratio are similar to those of basaltic glass–ceramics obtained from fused rocks. However, the reducing conditions in the batch must be adjusted in order to reach an approximate ratio $Fe^{3+}/Fe^{2+} = 2$. Sugar was not efficient as a reducing agent because it volatilized at low temperatures. Coal will be tested as a possible alternative.

Application of the FFD method to glass crystallization allowed us to reduce the experimental tests with the same degree of accuracy at a full factorial design. Moreover, by FFD analysis the influence of each experimental factor and their interactions on the glass crystallization process were highlighted. Using the surface response method, the analysis will be carried out to obtain the best experimental conditions which correspond to maximum crystallization.

Acknowledgements

The work is supported by the European Community under project MA2R-CT90-0007. The authors are grateful to Ms Fabiola Ferrante and Mr R. Pacione for their valuable contribution to the experimental work.

References

1. P. W. McMILLAN, "Glass ceramics" (Academic, London, 1979) p. 168.
2. J. HLAVAC, "The technology of glass ceramics" (Elsevier, 1983).
3. Z. STRNAD, "Glass science and technology" (Elsevier, Amsterdam, 1986) p. 110.
4. M. PELINO, L. MARINACCI, C. CANTALINI and P. P. BOATTINI, *Advanced Ceram. Glass* **4** (1992) 13.
5. M. PELINO, C. CANTALINI, P. P. BOATTINI, C. ABBRUZZESE and J. Ma. RINCON, in Proceedings of Austceram 92, edited by M. J. Bannister, Melbourne, August 1992, p. 1173.
6. M. PELINO, C. CANTALINI, P. P. BOATTINI, C. ABBRUZZESE, J. Ma. RINCON and J. E. GARCIA HERANDEZ, in proceedings of EMRS 1992 Fall Meeting, Strasbourg, November, 1992.
7. *Idem, Resources, Conservation & Recycling* in press.
8. J. Ma. RINCON, P. CALLEJAS and M. ROMERO, 2nd Semestral Report, EC Contract MA2R-CT90-000 7 (DG, XII, Bruxelles, 1993).
9. G. H. BEALL and H. L. RITTER, *Amer. Ceram. Soc. Bull.* **55** (1976) 579.
10. M. RUTSTEIN, *Amer. Min.* **54** (1968) 238.
11. O. L. DAVIES, "The design and analysis of industrial experiments" (Longman, London, 1979) p. 440.

Received 1 February
and accepted 8 July 1993